The 2010 IEEE/RSJ International Conference on
Intelligent Robots and Systems
October 18-22, 2010, Taipei, Taiwan

Study of the Relationship Between the Strain and Strain Rate for Viscoelastic Contact Interface in Robotic Grasping

Chia-Hung Dylan Tsai, Jun Nishiyama and Imin Kao
Department of Mechanical Engineering
SUNY at Stony Brook, Stony Brook, USA

Mitsuru Higashimori and Makoto Kaneko
Department of Mechanical Engineering
Osaka University, Osaka, Japan

***Abstract*— In this paper, a nonlinear latency model is presented to describe the relationship between the strain and strain rate of the temporal responses in robotic grasping that involves viscoelastic contact interface. The results from experiments and simulation are presented, and are found to match well with each other. The nonlinear latency model was able to adequately represent both Type I and Type II relaxation responses. For the successive loading and holding with a soft contact, the model describes the behavior of step-wise increase of equilibrium strain and a polynomial relationship between the strain rate and the strain. The nonlinear latency model can successfully predict and model the behavior of anthropomorphic soft contact interface in grasping and manipulation when the grasped object is held in certain posture of prehension with repeated loading and/or unloading.**

I. INTRODUCTION

Viscoelastic materials display the properties of both elastic solids and viscous fluids. As a result, viscoelastic materials exhibits both elastic (linear or nonlinear) response and temporal response when subject to external stimuli, such as force or displacement. Most biological materials are considered viscoelastic. Viscoelastic materials exhibits two important temporal responses when subject to displacement and force in contact interface. They are *stress relaxation* and *strain creep*, respectively. In this paper, the nonlinear relationships between the strain and strain rate of viscoelastic materials are studied and derived based on the linear latency model presented in [25]. Furthermore, simulation studies using the latency model also produce results of stress relaxation and strain creep responses that correlate well with the experimental data.

A. Literature review

Research studies have been conducted on the dynamic behavior of viscoelastic materials, especially the stress wave propagation. Theocaris and Papadopoulou studied the propagation of stress waves in viscoelastic media based on the Kelvin-Voigt model [20]. Turhan and Mengi proposed three types of inhomogeneities of the stress wave within the viscoelastic media [28]. Stucky and Lord utilized the finite element modeling method (FEM) to analyze the properties of ultrasonic waves in linear viscoelastic media [18]. Pereira, Mansour and Davis employed a wave propagation technique to measure the dynamic viscoelastic properties of excised skin when subjected to a low incremental strain [15]. Fowles and Williams derived two different phase velocities from conservation relations, mass and energy [5]. The study of viscoelasticity has benefited from different perspectives over the decades. The Maxwell model and the Kelvin-Voigt model are the first models used to describe the behavior of viscoelasticity [4]. After that, the generalized Maxwell model was proposed and has been widely used in modeling of linear viscoelasticity. Sakamoto *et. al* applied the modified spring-damper model to the grasping analysis of viscoelastic materials in [16]. Many other studies of viscoelastic behaviors were presented in [14], [8], [17], [2], [13], [19], [9], [10]. Research of viscoelasticity also has been done from the rheology viewpoint [12], [3], [1]. Golik proposed a model based on the diffusion of holes inside rubber under an external force [7]. Contrary to the Maxwell model which uses linear springs and dampers, Fung proposed an empirical model that separates elastic and temporal responses [6]. Tiezzi and Kao adopted Fung's approach to model the soft contact [22], [24], [21], [23], [11], [30], [29]. The consistency of the parameters in Fung's model has been illustrated [26]. This is in contrast to the Maxwell model and other related models that can render differences in the values of springs and dampers (for the same material at the same location) on one or two order of magnitude—a result that is not intuitive and may be contradictory to the concept of linear device modeling.

Tsai and Kao proposed the *latency model* which postulates that the stress relaxation can be considered as a result of uneven strain distribution before the material reaches a new equilibrium state [25]. Furthermore, Tsai and Kao utilized the latency model to explain the responses under different loading rates of external force [27], in which different responses are shown to be a result of different loading rates due to the temporal effect of viscoelasticity.

B. Relaxation and creep responses of viscoelasticity

Stress relaxation and strain creep are two well-known properties of viscoelastic materials. Stress relaxation, normally called *relaxation*, depicts the varying contact force/stress with time when a constant displacement is applied to the material [6]. Two types of relaxations are defined in [25] and shown in Figure 1. Type I relaxation exhibits decreasing stress under a constant displacement, typically at the end of loading. Type II relaxation exhibits increasing stress under a constant displacement, typically at

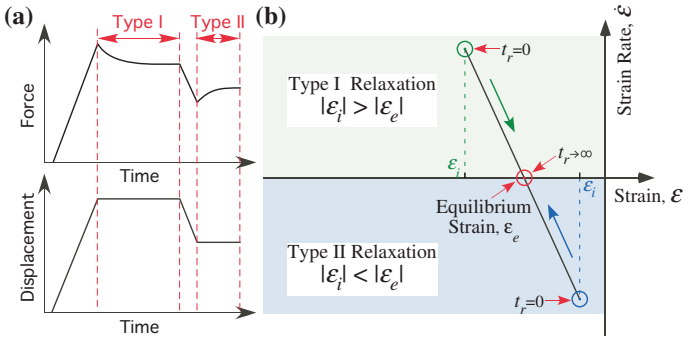

Fig. 1. (a) Type I and Type II relaxation as observed experimentally in association with the latency model. (b) The latency model with linear relationship between strain and strain rate [25].

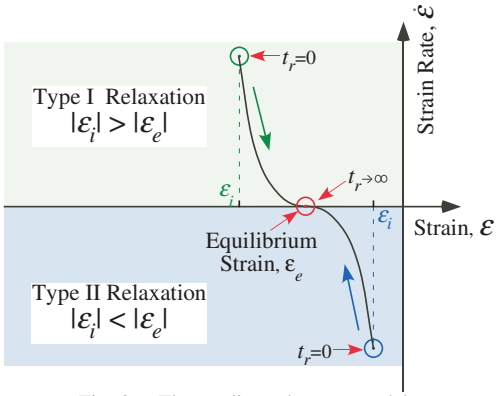

Fig. 2. The nonlinear latency model

the end of unloading. (See Fig. 1.) Creep response, the other important property, is the displacement/strain change when a constant force is applied to viscoelastic materials. Creep and relaxation illustrate the delayed temporal responses with the application of displacement or force.

C. Applications

The study of viscoelastic responses is important because of its relevance to both the stability and the response of contact interface in robotic grasping and manipulation. Furthermore, the results of such study can be used to optimize energy consumption for robotic grasping by understanding the nature of viscoelastic contact interface, and to facilitate the modeling of robotic grasping which involves both elastic and temporal responses, such as those in soft fingers, biomedical tissues, and anthropomorphic contact interface.

II. Theoretical Background

Based on the experimental observation and the fundamental concept in physics, we postulate the following two aspects of viscoelastic contact behaviors.

1) The two viscoelastic phenomena, stress relaxation and strain creep, are caused by unbalanced stress states within the material subject to transition of external stimuli. Such response in some literature was referred to as hole displacement, especially in polymeric materials [7]. The velocity of stress propagation inside the material determines the time constants of exponential decay or growth for stress relaxation or strain creep.
2) The material, given enough time, will always approach the equilibrium state at which internal stress is balanced and stress propagation ceases. This state is called the equilibrium state.

The latency model [25] proposed by Tsai and Kao is described by the following equations

$$\dot{\varepsilon}_c = -\nu_1(\varepsilon_c - \varepsilon_e) \quad \& \quad \varepsilon_e = -\frac{N_0 c_0}{\alpha_c} \tag{1}$$

where ε_c is the compressive strain measured externally at the contact interface, $\dot{\varepsilon}_c$ is the strain rate, and ε_e is the strain when equilibrium state is reached. The parameters ν_1, N_0, c_0 and α_c are constants pertaining to material properties [25].

The latency model elucidates a process for viscoelastic materials to reach equilibrium after being subjected to external stimuli. When a new equilibrium state is reached, the strain becomes the equilibrium strain, $\varepsilon = \varepsilon_e$, with the strain rate becoming zero, $\dot{\varepsilon} = 0$. In [25], stress relaxation was discussed and modeled by assuming one exponential term in the exponentially decaying temporary response. Based on the latency model with this assumption, an intuitive and straightforward linear relationship (with a closed-form solution) between the strain and strain rate can be obtained, as shown in Fig. 1. The temporal response in Fig. 1 is a function of the time t, with $0 \le t \le \infty$.

The experimental results suggest that the relationship is nonlinear, as shown in the nonlinear latency model in Fig. 2. As a result, we propose the following empirical model to represent the nonlinear polynomial relationship between the strain and strain rate in the following equations with respect to odd or even exponent

$$\dot{\varepsilon} = \begin{cases} -\nu(\varepsilon - \varepsilon_e)^n & \text{if } n \text{ is odd} \\ -[\mathrm{sgn}\,(\varepsilon - \varepsilon_e)]\nu(\varepsilon - \varepsilon_e)^n & \text{if } n \text{ is even} \end{cases} \tag{2}$$

where ε_e is the equilibrium strain, ν and n are constants of the empirical polynomial function, and ε is the instantaneous strain at any point within the material. Eq. (2) shows that the magnitude of strain rate can be determined from the current strain, ε, and the equilibrium strain, ε_e. In other word, if the current strain is further away from the equilibrium strain, a larger magnitude of strain rate will be expected.

In this paper, we adopt odd exponents in equation (2) for the convenience in analysis. With n being odd, we can rewrite (2) as follows

$$\dot{\varepsilon} = -\nu(\varepsilon - \varepsilon_e)^n \tag{3}$$

Eqs. (2) and (3) extends the linear model in Fig. 1 to include the nonlinearity observed in experiments. The experimental study will be presented in Section III. This model has two assumptions. First, the material is assumed to be homogeneous. Second, every infinitesimal element within the material is assumed to have similar property, such that we can apply the empirical model from the exterior contact surface to the core of the material.

The solution of the differential equation in (3), before reaching the equilibrium state ε_e, can be obtained as follows.

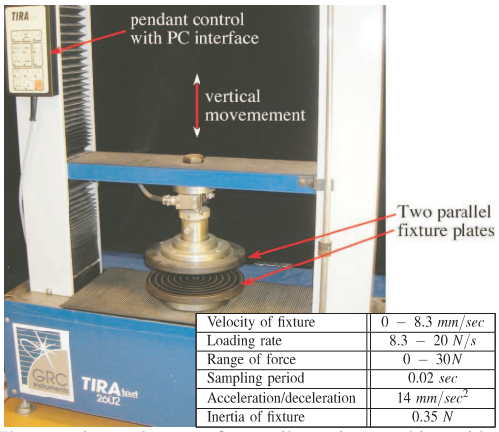

Velocity of fixture	$0 - 8.3\ mm/sec$
Loading rate	$8.3 - 20\ N/s$
Range of force	$0 - 30N$
Sampling period	$0.02\ sec$
Acceleration/deceleration	$14\ mm/sec^2$
Inertia of fixture	$0.35\ N$

Fig. 3. The experimental setup of a tensile testing machine with a pair of flat parallel fixture plates.

(I) When $\varepsilon_e > \varepsilon_0$:

$$\varepsilon = \varepsilon_e - [(n-1)(\nu t + c)]^{\frac{1}{1-n}} \quad \text{with} \quad c = \frac{(\varepsilon_e - \varepsilon_0)^{1-n}}{(n-1)} \tag{4}$$

(II) When $\varepsilon_e < \varepsilon_0$:

$$\varepsilon = \varepsilon_e + [(n-1)(\nu t + c)]^{\frac{1}{1-n}} \quad \text{with} \quad c = \frac{(\varepsilon_0 - \varepsilon_e)^{1-n}}{(n-1)} \tag{5}$$

where $\varepsilon_0 = \varepsilon(0)$ is the boundary condition, which represent the initial strain when $t = 0$.

Eqs. (4) and (5) are the solutions of the differential equation of the nonlinear latency model. The solutions of the strain ε is a function of time, the exponent n, and the coefficient ν. When $t \to \infty$, the second term on the right-hand side of the equal sign will vanish, resulting in $\varepsilon = \varepsilon_e$. Physically, this means that the strain will converge asymptotically to an equilibrium strain when time approaches infinity. This is consistent with the latency model and observation based on the experimental data.

III. EXPERIMENTAL STUDY

A tensile test machine is employed to conduct experiments for measuring and observing the temporal responses of viscoelastic contact interface. The experimental setup and procedures are explained in the following sections.

A. Experimental Setup

Experiments were conducted using a tensile testing machine with a pair of parallel flat fixtures pressing upon the object, as shown in Fig. 3. The system is identical to a parallel-jaw gripper, and will be so referred to in this paper. The load cell has a range of $2\,kN$ force with an accuracy of $0.2\,N$ and high repeatability. The displacement measurements have an accuracy of $10^{-3}\,mm$. Multiple experiments with varying loading rates, stationary and relaxation phase, and unloading phase were conducted. The parameters of the experiments are tabulated in Fig. 3.

The inertia of the fixture is compensated by the design of the equipment in order to minimize the effect of force measurement due to acceleration or deceleration. Calibration experiments were conducted to measure the inertia force without contact to identify the amount of inertia force due to the fixture alone. The results indicate a maximum of $0.35\,N$ of inertia force (within the range of acceleration and deceleration used in the experiments) measured by the load cell, which is only slightly larger than the accuracy of the load cell. Based on the parameters used in the experiments, we conclude that the inertia effect is less than 1% of the typical range of forces; therefore, it is negligible.

The material of the grasped object is a viscoelastic soft rubber ball with a radius of $35\,mm$.

B. Procedures of Experiments

The procedures of various experiments conducted with different loading rates are enumerated in the following.

1) The gripper is moved to barely touch the surface of the viscoelastic object.
2) The upper fixture moves in vertical direction for loading, unloading, and holding by following a prescribed control sequence of displacements.
3) The gripper unloads and breaks contact.

Two different tests were conducted. In the first test, as shown in Fig. 4(a), the fixture moves to compress the viscoelastic object in an increment of $5\,mm$ with the displacements of 5, 10, 15, 20, and $25\,mm$. At the end of each loading sequence and increment, the fixture was held at that displacement for 10 seconds. This is shown in the bottom plot of Fig. 4(a). In the other test, the fixture first compressed the object to a displacement of $25\,mm$. After that, the displacements were reversed to go through the descending order of 25, 20, 15, 10, and $5\,mm$. The fixture was also held at each displacement for 10 seconds at every step and with the same loading/unloading rate, $500mm/min$. This is shown in the bottom plot of Fig. 4(b).

C. Experimental Results and Analysis

The experimental results of the two tests are presented in Figs. 4(a) and 4(b). The normal forces at the contact surface are measured and plotted in the top plots in Figs. 4(a) and 4(b).

To obtain strains and strain rates from the experimental results, we assume a linear relationship between the strain, ε, and stress, σ, for the sake of convenience in analysis; that is,

$$\varepsilon = \frac{\sigma}{E} = \frac{f/A}{E} \tag{6}$$

where A is the area of contact at the exterior surface, f is the measured force, and E is the Young's modulus of the material which has an average value of $2.8 \times 10^4\,Pa$. The area of contact grows with the amount of depression, d, of the fixture onto the surface of the object, and can be written as follows

$$A = \pi a^2 = \pi[(r)^2 - (r-d)^2] \tag{7}$$

where r is the radius of the ball, a is the radius of the contact area, and d is the displacement (or depression) in the vertical direction, as shown in Fig. 5

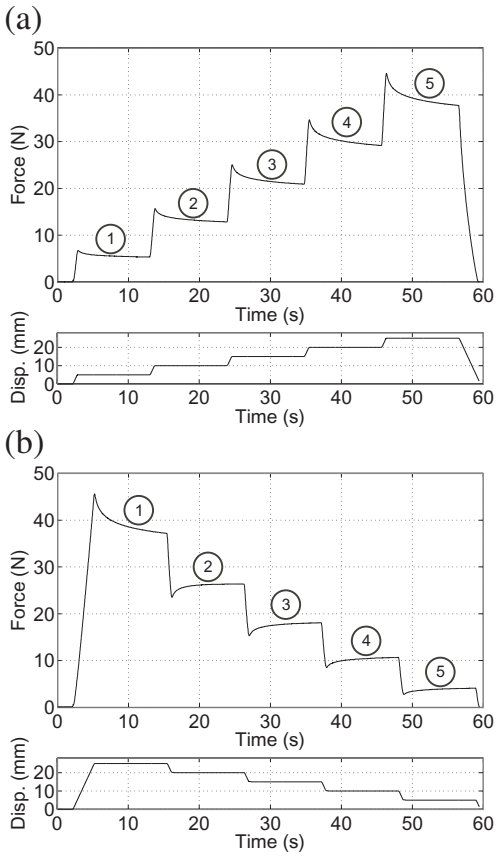

Fig. 4. Experimental results from a tensile test with a pair of flat parallel fixture plates. (a) loading and relaxation; (b) loading followed by successive unloading and hold. Bother Types I and II relaxation are present.

Finally, we can calculate the strains and strain rates as functions of time

$$\varepsilon(t) = \frac{f(t)}{E\pi[r^2-(r-d(t))^2]} \quad (8)$$

$$\dot{\varepsilon}(t) = \frac{d\varepsilon(t)}{dt} \quad (9)$$

The strains and strain rates can be calculated based on the measured force and displacement, and are plotted as blue curves in Fig. 6(a) and Fig. 6(b).

Next, we chose $n=5$ in (2) because it is the lowest order of polynomial which fits the experimental results the best. The nonlinear latency model becomes

$$\dot{\varepsilon} = -\nu(\varepsilon-\varepsilon_e)^5 \quad (10)$$

The least-square (LS) curve fitting technique is applied using Eq. (10) with the results plotted as red curves in Fig. 6(a) and Fig. 6(b). The parameters are listed in Table I for loading and Table II for unloading.

The fitting results indicate that the equilibrium strains, ε_e, are consistent for the same displacement in both continuous loading and continuous unloading experimental results. In addition, we found that the parameter, ν, in the continuing loading experiment in Table I shows consistent decrease with the increase in corresponding equilibrium strain, ε_e. This trend, however, is not repeatable in unloading (Table II).

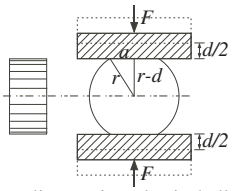

Fig. 5. A model of a nonlinear viscoelastic ball making contact with a parallel-jaw gripper. The contact area is assumed to be circular. The plot to the left of the grasped object is the plot of equivalent latency model.

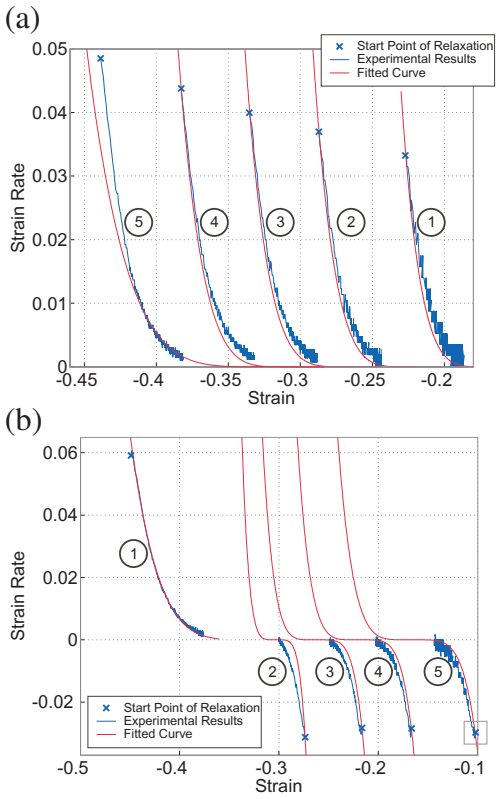

Fig. 6. Plots (a) and (b) are the analysis of strain rate versus strain of the experimental results (a) and (b) in Fig. 4, respectively. The blue points are the values calculated from the experimental results, using (6) and (7). The red curves are the best fit using (10).

It may be due to the different mechanisms of loading and unloading. For loading, the test machine gave a direct displacement for compression. But for unloading, the gripper moved backward and let material expand freely. We believe this may be a reason for the inconsistent phenomenon of ν between the two sets of parameters in Tables I and II.

IV. SIMULATION

Based on the model presented in (2), we use MATLAB to simulate the force response with the same displacement profile as that in the experiments, shown in Figs. 4(a) and 4(b). As the fixture of the tensile machine moves the distance of d, the movement is kinematically identical to each contact surface moving with a distance of $d/2$, with respect to the plane of symmetry in the middle of the ball, as illustrated in Fig. 5. The procedures of simulation are presented in the next section.

TABLE I

FITTING RESULTS OF FIG. 6(A) (LOADING) $\dot{\varepsilon} = -\nu(\varepsilon - \varepsilon_e)^5$

curve #	1	2	3	4	5
ε_e	-0.1661	-0.2193	-0.2623	-0.3031	-0.3144
ν	4.1×10^4	2.6×10^4	2.0×10^4	1.4×10^4	1.2×10^3

TABLE II

FITTING RESULTS OF FIG. 6(B) (UNLOADING) $\dot{\varepsilon} = -\nu(\varepsilon - \varepsilon_e)^5$

curve #	1	2	3	4	5
ε_e	-0.3144	-0.3031	-0.2623	-0.2193	-0.1661
ν	1.4×10^3	1.4×10^6	1.4×10^5	7.0×10^4	2.8×10^4

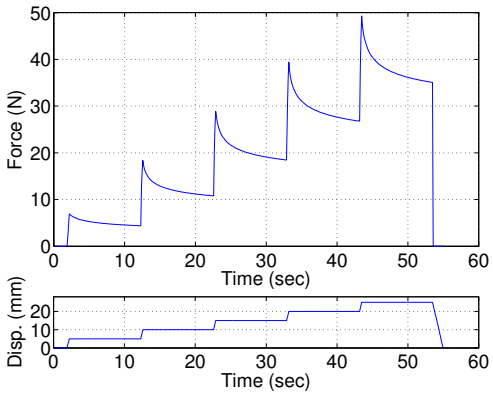

Fig. 8. The results of simulation corresponding to Fig. 4(a).

A. Simulation Procedures

1) First, we divide the material into m segments axially, as illustrated in Fig. 7.
2) The displacement of contact surface is updated with the progress of compression. We assume the displacement will eventually be evenly distributed when time approaches infinity. As a result, the equilibrium strain, ε_e at the i-th element equals the displacement of i-th node divided by the original length from i-th node to the symmetric center.
3) The model in (10) is applied to each of the segments from the contact element from the exterior surface to the plane of symmetry. The strain of each element changes according to the corresponding strain rate calculated by (10).
4) The force at the contact interface will simply be equal to the product of the stress at the contact interface, σ_1 (the first element), and the contact area, A. That is,

$$F = \sigma_1 \times A = (E\varepsilon_1) \times \left\{\pi[r^2 - (r-d_1)^2]\right\} \qquad (11)$$

B. Simulation Results

Fig. 8 shows the results of simulation based on the model presented in (10), corresponding to the experimental results in Fig. 4(a). The procedures of simulation are described in the previous section. It can be seen from the results that the trend of Type I relaxation in simulation is similar to that of the experimental results. In addition, the amount of relaxation in each step also matches quite well with the experimental data in Fig. 4(a). This suggests that the proposed model can capture the relaxation responses of such grasping task adequately. We note that the unloading curve at the end of Fig. 8 (at $t \cong 53\,sec$) drops faster than the experimental results, which is probably due to the different mechanisms in loading and unloading as discussed in the end of the previous section. Overall, the simulation employed here can capture the relaxation responses of successive loading, and can model the nonlinear latency response well. This simulation tool will be useful in studying the robotic grasping or prehension that involves soft viscoelastic contacts.

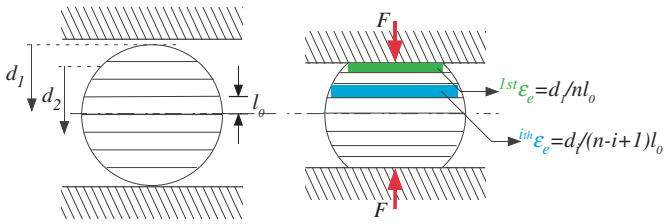

Fig. 7. This diagram shows the discrete model used in the simulation. The object is divided into m segments ($m = 8$ in this figure). When an external force, F, is applied, the stress/strain wave will propagate toward the plane of symmetry of the grasped object, consistent with the latency model illustrated in Figure 5. In order to apply the model in (10) to the simulation, we estimate the equilibrium strain, $^{ith}\varepsilon_e$, of the i-th element by assuming the strain between the i-th element and plane of symmetry is uniformly distributed.

V. DISCUSSIONS

Based on the preceding presentation of the results of experimental study and simulation using the nonlinear latency model, observation and results are presented in the following.

A. Amount of relaxation versus displacement

As experimental results in Fig. 4(a) and Fig. 4(b) show, a larger amount of relaxation is always resulted when the displacement of loading is larger. This is due to the higher equilibrium strain, ε_e.

B. Results in Tables I and II

In Table I, it is observed that the magnitudes of the equilibrium strain, $|\varepsilon_e|$, increases as the loading-holding procedure repeats itself from steps 1 to 5. This causes a larger amount of relaxation, as alluded to in Section V-A. In addition, the values of the coefficient, ν, decreases as the loading-holding process progresses from steps 1 to 5. It is also noted that with the increase of the magnitude of the equilibrium strain, $|\varepsilon_e|$, the coefficient, ν, decreases.

In Table II, it is observed that the magnitudes of the equilibrium strain, $|\varepsilon_e|$, decreases as the unloading-holding procedure repeats itself from steps 2 to 5, after the initial loading to the maximum displacement of $25\,mm$. The values of the coefficient, ν, decreases when the unloading-holding cycles start after step "2". (Step 1 is the loading process.) The values of the equilibrium strains at the various displacement steps are the same as the corresponding ones in Tables I.

VI. CONCLUSIONS

In this paper, a contact model for nonlinear viscoelastic materials is presented with both simulation and experiments. The model describes the relationship between the strains and the strain rates of infinitesimal element within the material. The proposed model postulates that the values of strain will asymptotically reach an equilibrium strain. The nonlinear latency model attempts to characterize the path by which the strain varies from the initial value to the equilibrium strain, with successive loading, unloading, and holding—a situation which occurs often in robotic grasping and manipulation involving soft contacts. The simulation tool developed based on the latency model appears to match well with the experimental results.

Future study will be focused on the physical meaning of the exponent, n, of the nonlinear latency model and its correlation to the material structure or property of soft contacts.

VII. ACKNOWLEDGEMENT

This research has been supported by the NSF (National Science Foundation) Grant CMMI0800241, as well as a collaborative joint grant from JST H19/299-1 (Japan Science and Technology Agency).

REFERENCES

[1] D. B. Adolf, R. S. Chambers, and J. Flemming. Potential energy clock model: Justification and challenging predictions. *Journal of Rheology*, 51(3):517–540, 2007.

[2] F. Barbagli, A. Frisoli, K. Salisbury, and M. Bergamasco. Simulating human fingers: a soft finger proxy model and algorithm. In *Proc. IEEE Int. Symp. on Haptic Interface, HAPTICS'04*, 2004.

[3] W. N. Findley and J. S. Y. Lay. A modified superposition principle applied to creep of non-linear viscoelastic material under abrupt changes in state of combined stress. *Trans. of the Society of Rheology*, vol. 11(3):361–380, 1967.

[4] W. Flugge. *Viscoelasticity*. Blaisdell Publishing Company, 1967.

[5] R. Fowles and number = 1 year = 1970 pages = 360 - 363 R. F. Williams), volume = 41. Plane stress wave propagation in solids. *Journal of Applied Physics*.

[6] Y. C. Fung. *Biomechanics: Mechanical Properties of Living Tissues*. Springer-Verlag, 1993.

[7] A. Z. Golik and Y. F. Zabashta. a molecular model of creep and stress relaxation in crystalline polymers. *Mekhanika Polimerov*, pages 969–975, 1971.

[8] R. D. Howe, N. Popp, I. Kao, P. Akella, and M. R. Cutkosky. Grasping, manipulation, and control with tactile sensing. In *Proc. IEEE Int. Conf. on Robotics and Automation, ICRA*, Cincinnati, OH, 1990.

[9] T. Inoue and S. Hirai. Elastic model of deformable fingertip for soft-fingered manipulation. *IEEE Trans. in Robotics*, 22:1273–1279, 2006.

[10] T. Inoue and S. Hirai. Quasi-static manipulation using hemispherical soft fingertips by means of minimum d.o.f. two-fingered robotic hand. *J. of the Robotics Society of Japan*, 24:945–953, 2006.

[11] I. Kao and F. Yang. Stiffness and contact mechanics for soft fingers in grasping and manipulation. *the IEEE Trans. of Robotics and Automation*, 20(1):132–135, February 2004.

[12] M. Kimura, Y. Sugiyama, S. Tomokuni, and S. Hirai. Constructing rheologically deformable virtual objects. In *Proc. IEEE Int. Conf. on Robotics and Automation, ICRA*, pages 3737–3743, 2003.

[13] Y. Li and I. Kao. A review of modeling of soft-contact fingers and stiffness control for dextrous manipulation in robotics. In *Proc. IEEE Int. Conf. on Robotics and Automation, ICRA*, pages 3055–3060, Seoul, Korea, 2001.

[14] D. T. V. Pawluk and R. D. Howe. Dynamic contact of the human fingerpad against a flat surface. *ASME Jour. of Biomechanical Engineering*, vol. 121(6):605–611, 1999.

[15] J.M. Pereira, J.J. Mansour, and B.R. Davis. Dynamic measurement of the viscoelastic properties of skin. *Journal of Biomechanics*, 24(2):157 – 162, 1991. Collagen Network;Dynamic Wave Propagation Method;Proteoglycan Gel;Skin Strain Properties;Skin Viscoelastic Properties;.

[16] N. Sakamoto, M. Higashimori, T. Tsuji, and M. Kaneko. An optimum design of robotic hand for handling a visco-elastic object based on maxwell model. In *Proc. IEEE Int. Conf. on Robotics and Automation, ICRA 2007*, pages 1219–1225, Roma, Italy, April 10-14 2007.

[17] K. B. Shimoga and A. A. Goldenberg. Soft robotic fingertips - part I and II: A comparison of construction materials. *Int. Jour. of Robotic Research*, 15(4), 1996.

[18] Paul Stucky and William Lord. Finite element modeling of transient ultrasonic waves in linear viscoelastic media. *IEEE Transactions on Ultrasonics, Ferroelectrics, and Frequency Control*, 48(1):6 – 16, 2001. Linear viscoelastic media;.

[19] H. Takagi, M. Takahashi, R. Maeda, Y. Onishi, Y. Iriye, T. Iwasaki, and Y. Hirai. Analysis of time dependent polymer deformation based on a viscoelastic model in thermal imprint process. *Microelectronic Engineering*, 85:902–906, 2008.

[20] P.S. Theocaris and N. Papadopoulou. Propagation of stress waves in viscoelastic media. *Polymer*, 19(2):215 – 219, 1978.

[21] P. Tiezzi and I. Kao. Characteristics of contact and limit surface for viscoelastic fingers. In *IEEE Int. Conf. on Robotics and Automation, ICRA 2006*, pages 1365–1370, Orlando, Florida, May 15-19 2006.

[22] P. Tiezzi and I. Kao. Modeling of viscoelastic contacts and evolution of limit surface for robotic contact interface. *IEEE Transaction on Robotics*, 23(2):206–217, April 2007.

[23] P. Tiezzi, I. Kao, and G. Vassura. Effect of layer compliance on frictional behavior of soft robotic fingers. In *Proc. IEEE Int. Conf. on Intelligent Robots and Systems (IROS 2006)*, pages 4012–4017, Beijing, China, October 2006.

[24] P. Tiezzi, I. Kao, and G. Vassura. Effect of layer compliance on frictional behavior of soft robotic fingers. *Advanced Robotics*, 21(14):1653–1670, 2007.

[25] C. D. Tsai and I. Kao. The latency model for viscoelastic contact interface in robotics: Theory and experiments. In *Proc. 2009 IEEE Int. Conf. on Robotics and Automation (ICRA 2009)*, pages 1291–1296, Kobe, Japan, May 2009.

[26] C. D. Tsai, I. Kao, N. Sakamoto, M. Higashimori, and M. Kaneko. Applying viscoelastic contact modeling to grasping task: an experimental case study. In *International Conference on Intelligent Robots and Systems, IROS*, pages 3737–3743, 2008.

[27] C. D. Tsai, I. Kao, K. Yoshimoto, M. Higashimori, and M. Kaneko. An experimental study and modeling of loading and unloading of nonlinear viscoelastic contacts. In *International Conference on Intelligent Robots and Systems, IROS*, pages 3737–3743, October 2009.

[28] D. Turhan and Y. Mengi. Propagation of initially plane waves in nonhomogeneous viscoelastic media. *International Journal of Solids and Structures*, 13(2):79 – 92, 1977. NONHOMOGENEOUS VISCOELASTIC MEDIA;WAVE PROPAGATION;.

[29] N. Xydas and I. Kao. Modeling of contacts and force/moment for anthropomorphic soft fingers. In *Proc. of Int. Conf. on Intelligent Robots and Systems, IROS*, pages 488–493, Victoria, Canada, 1998.

[30] N. Xydas and I. Kao. Modeling of contact mechanics and friction limit surface for soft fingers in robotics, with experimental results. *Int. J. of Robotic Research*, 18(8):941–950, 1999.